Reports

A Search for Iridium Abundance Anomalies at Two Late Cambrian Biomere Boundaries in Western Utah

Abstract. *Iridium concentrations have been measured in samples taken across two Late Cambrian biomere boundaries (crisis zones) in search of evidence for possible elemental abundance anomalies similar to the one observed at the Cretaceous-Tertiary boundary. Sampling was performed in uplifted marine limestone deposits in the House Range of western Utah. Although the two trilobite-brachiopod extinction boundaries could be assigned to ±4 millimeters of vertical section by laboratory examination of the rocks, only background amounts of iridium* (2×10^{-12} *to* 17×10^{-12} *gram per gram of whole rock) were observed.*

After the initial reports by Alvarez *et al.* (*1*) of an iridium abundance anomaly in sediments corresponding to the Cretaceous-Tertiary (K/T) boundary, there accumulated a significant body of geochemical evidence (*2, 3*) indicating that the iridium enrichment pulse is a global phenomenon stemming from a single event. Alvarez *et al.* proposed that this event was the earth impact of an asteroid of the order of 10 km in diameter, which ejected into the stratosphere sufficient dust to darken the earth for several months, producing the biological crisis that defines the end of the Cretaceous period. Relative to its concentration in most classes of meteorites, iridium is depleted in the earth's crust by three to four orders of magnitude.

Investigators of the size and time distribution of lunar and terrestrial impact craters and of earth-crossing asteroids and comets (*4*) have concluded that asteroidal objects as large as 10 km in diameter probably collide with the earth every 50×10^6 to 100×10^6 years, and comet nuclei of similar size may have comparable collision rates. Thus, we might expect to find several more significant iridium anomalies in strata laid down since the early Cambrian (about 570×10^6 years ago). Obvious zones in which to search would be at other extinctions in the fossil record, of which there are known to be at least four (*5*). Ganapathy (*6*), Alvarez *et al.* (*7*), and Asaro *et al.* (*8*) have recently reported an iridium anomaly that is associated with microtektites and with the radiolarian extinction zone that marks the marine Eocene-Oligocene boundary about 34×10^6 years ago.

We describe here some paleontologic observations and geochemical measurements, including iridium assays, across both boundaries of the Late Cambrian Pterocephaliid biomere: the Marjumiid-Pterocephaliid boundary (M/P) and the Pterocephaliid-Ptychaspid boundary (P/P) (Fig. 1). At several Nevada and Utah localities, where the rocks are especially fossiliferous, these boundaries are well documented (*9, 10*). These biostratigraphic boundaries are characterized by an abrupt extinction of assemblages of trilobites that had been highly diverse and evidently well adapted and their replacement by a low-diversity fauna dominated by only one or two species, all within a few centimeters of section. The pattern of extinction is similar to that of the calcareous plankton at the K/T boundary (*3*) and was considered to offer another possible example of an impact-related biological crisis (*9*).

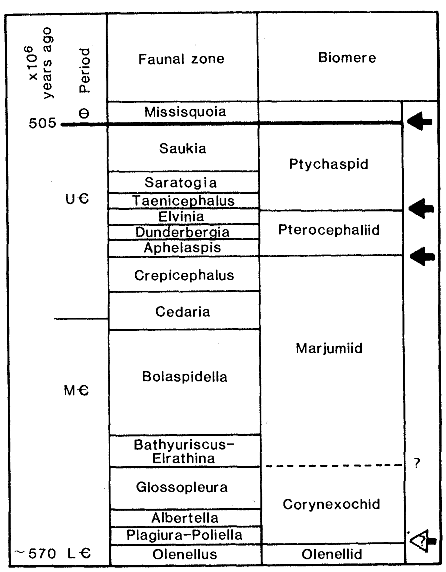

Fig. 1. Stratigraphic position of documented (solid arrows) and suspected (open arrow or question mark) biomere boundary events in the Cambrian system of North America. The upper and lower boundaries of the Pterocephaliid biomere were examined in this work. Under period, Θ, *U€*, *M€*, and *L€* correspond to Ordovician, Upper Cambrian, Middle Cambrian, and Lower Cambrian, respectively.

We conducted our search at several sites in and above Little Horse Canyon in the House Range of western Utah, where M/P and P/P biomere boundaries are exposed. These exposures are uplifted marine limestone beds deposited about 520×10^6 years ago near the outer margin of a shallow epicontinental sea. Paleomagnetic and paleogeographic studies by Bambach *et al.* (*11*) have indicated that at that time the ancestral North American continent straddled the equator.

Two suites of samples were taken, one involving three passes across the M/P biomere boundary and spanning 50 cm of vertical section and the second across the younger (about 5×10^6 years) P/P boundary and spanning 120 cm. Slices were cut from our primary limestone sample blocks for laboratory paleontologic examination. Parallel sample sequences were taken for geochemical measurement: a total of 100 samples was analyzed for iridium and a dozen other elements by means of instrumental neutron activation analysis, and 47 of these irradiated samples were dissolved and radiochemically processed to isolate the activated iridium, providing a hundredfold improvement in detection sensitivity.

Data for our most detailed section across the M/P biomere boundary are summarized in Table 1 and displayed in Fig. 2A. The boundary was bracketed vertically to about ±1 cm by field examination of these beds. Later laboratory examination established the boundary to within a few millimeters, as indicated in Fig. 2A. The iridium concentrations in these samples are very low, typically of the order of $(4 \pm 1) \times 10^{-12}$ g per gram of whole rock (= 4 pg/g), similar to average crustal concentrations. We obtained similar results from two additional measured sections across this zone taken at other locations within a lateral distance of 100 m. The iridium concentration in the boundary sample (Fig. 2A) is about three times the average of the others in this section; the other two sections exhibited no such irregularity at the boundary, but one of them showed a value of 18 pg per gram of whole rock 40

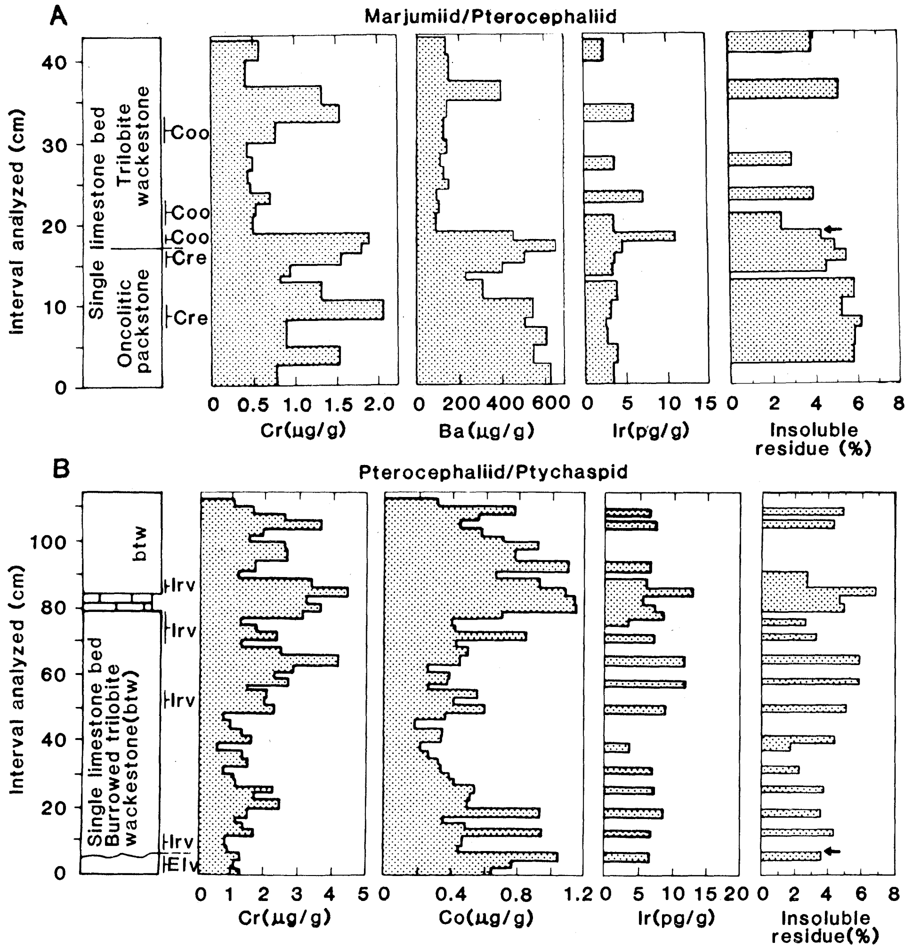

Fig. 2. Whole-rock elemental abundances and percentages (by weight) of insoluble residue after treatment with $2M$ HNO_3. The M/P boundary (A) is indicated by the line at 17 cm that separates the highest occurrence of *Crepicephalus* (*Cre*) trilobites from the first appearance of *Coosella* (*Coo*). The P/P boundary (B) is indicated by the line at 5 cm that separates the highest occurrence of *Elvinia* (*Elv*) trilobites from the first appearance of *Irvingella* (*Irv*).

cm up-section. At these low concentrations, we consider such irregularities as lying within the normal range of variations and not indicative of an exotic event. Iridium concentrations at the marine K/T boundary are commonly reported to lie in the range 5000 pg per gram of acid-insoluble residue, with values up to 87,000 pg/g. Our iridium concentrations, expressed on the basis of acid-insoluble residue, range from 40 to 300 pg/g. The concentrations of chromium and barium decrease abruptly at the M/P biomere boundary, although calcium carbonate is the dominant constituent (80 to 95 percent) of the rock throughout the column.

Thus, although the M/P boundary is accompanied by small changes in the acid insolubles and in the element makeup, the geochemical data we have show no clear evidence of a catastrophe that could have brought about the observed extinction, particularly an extinction found in other localities hundreds of kilometers away.

For the P/P biomere boundary study we selected a site on Orr Ridge, stratigraphically about 228 m above the M/P boundary. On the basis of field examination for trilobite fragments, we chose a sampling interval centered about halfway between the last appearance of *Elvinia* and the unambiguous observation of *Irvingella* just above the rubble zone shown at 82 cm in Fig. 2B. Subsequent laboratory examination established the boundary about 45 cm below this provi-

Table 1. Whole-rock elemental abundances across the Marjumiid-Pterocephaliid biomere boundary; NR, not analyzed radiochemically; σ, standard deviation.

Sample location* (cm)	Mg (µg/g)	Ca (%)	Sc (µg/g)	Cr (µg/g)	Mn (µg/g)	Fe (%)	Co (µg/g)	Sb (ng/g)	Ba (µg/g)	La (µg/g)	Ir† (pg/g)	U (µg/g)
+23.0	7910	32.9	0.099	0.576	1990	0.108	0.319	12.3	140	0.74	2.0	0.10
+20.3	4000	35.5	0.128	0.404	1795	0.095	0.140	6.6	150	0.88	NR	0.19
+17.4	1500	35.0	0.280	1.391	1770	0.157	0.446	60.2	395	1.66	NR	0.32
+15.3	1430	35.7	0.362	1.570	1650	0.203	0.495	63.8	140	2.10	6.0	0.41
+12.8	1490	35.3	0.165	0.773	1767	0.115	0.318	38.3	145	1.16	NR	0.29
+10.7	1180	34.8	0.085	0.430	1419	0.065	0.174	10.8	110	0.89	NR	0.30
+9.0	1230	37.2	0.104	0.518	1192	0.086	0.277	25.3	120	0.99	3.4	0.23
+7.5	1070	37.6	0.112	0.465	1002	0.081	0.181	19.5	120	1.23	NR	0.25
+6.1	1380	40.4	0.102	0.480	936	0.075	0.133	41.5	160	1.30	7.8	0.16
+4.9	1210	35.1	0.163	0.726	1479	0.173	1.262	92.0	119	1.54	8.0	0.38
+3.5	1250	35.8	0.116	0.525	1217	0.095	0.330	30.2	120	1.08	NR	0.18
+1.8	2330	36.4	0.136	0.504	1218	0.103	0.223	16	130	1.45	2.5	0.17
0 (M/P)	1160	37.8	0.432	1.916	1210	0.166	0.873	69.6	458	2.13	11.0	0.43
−1.1	3610	34.6	0.393	1.822	1286	0.216	0.775	69.9	666	2.16	4.2	0.36
−2.4	5960	34.7	0.257	1.577	1338	0.244	1.060	90.8	509	1.70	3.7	0.24
−3.7	3870	35.0	0.219	0.955	1281	0.172	0.780	46.4	405	1.61	3.1	0.33
−4.7	3840	36.7	0.230	0.836	1357	0.262	1.100	76.5	230	1.74	NR	0.30
−6.3	3730	34.4	0.269	1.342	1280	0.204	2.758	71.3	310	1.62	3.7	0.43
−8.9	3060	33.9	0.268	2.086	1250	0.206	0.936	65.1	547	1.60	2.8	0.39
−10.2	12900	32.9	0.236	0.915	1402	0.333	0.535	82.1	508	1.67	2.2	0.29
−11.9	6120	36.1	0.301	0.914	1319	0.228	0.711	52.9	615	2.28	2.4	0.37
−14.1	6960	33.9	0.240	1.545	1272	0.245	1.455	69.6	547	1.83	3.6	0.43
−16.4	9080	32.5	0.227	0.781	1400	0.454	0.617	109.0	634	1.49	3.2	0.33
1 σ (%)	15	12	15	15	6	15	15	25	10	15	10	5

*The midpoint position of the sample is given in centimeters above (+) or below (−) the M/P boundary. †Detection sensitivity, 0.5 pg/g.

sional midpoint. It was marked by the abrupt disappearance of *Elvinia* and the appearance of *Irvingella*, accompanied by the disappearance of typical trilobites of the *Elvinia* zone and the associated acrotretid brachiopod *Linnarssonella* and the appearance of the distinctly different trilobite and brachiopod assemblage of the *Irvingella major* subzone. Here, as at the M/P boundary, our iridium data show no indication of a concentration anomaly, nor is there any obvious change in the amount of acid-insoluble residue or in the concentration ranges of the elements. However, thin-section analysis revealed a distinct hardground at the boundary, indicating a slight unconformity or hiatus. Thus, the absence of a geochemical anomaly could be a result of missing sediments.

In summary, we have found no significant iridium enrichments at either the M/P or the P/P biomere boundaries; the concentrations of this element are consistently in the range of picograms per gram of whole rock, the concentration characteristic of the earth's crust. Nor do the concentrations of any of the other elements measured exhibit exotic values. Impact of a large achondrite (known to contain less iridium than other meteorites) or of a comet would be less likely to produce an iridium signal detectable above crustal background. The dominant rock at both boundaries is limestone, with variations characteristic of terrestrial processes. Both of these biomere boundary sequences were deposited in shallow water, where wave and tidal action could have dissipated local concentrations of fallout material. Moreover, we have examined only one sampling site. Thus, although the iridium abundances that we have observed are typical of average crustal rock, we cannot definitely conclude that these two Cambrian extinctions were not associated with impacts of large extraterrestrial bodies. We believe that this possibility can be excluded only by iridium measurements on these two biomere boundaries at other distant locations characterized by abundant fossils and continuous deposition. There exist locations in the continental United States, for example, in Arizona, Texas, and Tennessee (*9*), that may prove suitable for these studies.

CHARLES J. ORTH
JERE D. KNIGHT
LEONARD R. QUINTANA
JAMES S. GILMORE
Los Alamos National Laboratory, Los Alamos, New Mexico 87545
ALLISON R. PALMER
Geological Society of America, Boulder, Colorado 80301

References and Notes

1. W. Alvarez, L. W. Alvarez, F. Asaro, H. V. Michel, *Eos* **60**, 734 (1979); L. W. Alvarez, W. Alvarez, F. Asaro, H. V. Michel, *Science* **208**, 1095 (1980).
2. W. Alvarez, L. W. Alvarez, F. Asaro, H. V. Michel, *Geol. Soc. Am. Spec. Pap. 190* (1982), p. 305; R. Ganapathy, *Science* **209**, 921 (1980); J. Smit and J. Hertogen, *Nature (London)* **285**, 198 (1980); F. T. Kyte, Z. Zhou, J. T. Wasson, *ibid.* **288**, 651 (1980); K. J. Hsü *et al.*, *Science* **216**, 249 (1982); C. J. Orth *et al.*, *ibid.* **214**, 1341 (1981); R. Ganapathy, S. Gartner, M.-J. Jiang, *Earth Planet. Sci. Lett.* **54**, 393 (1981); C. J. Orth *et al.*, *Geol. Soc. Am. Spec. Pap. 190* (1982), p. 423; J. Smit, *ibid.*, p. 329; M. A. Nazarov, L. D. Barsukova, G. M. Kolesov, D. P. Alekseev, V. I. Vernadsky, *Abstr. 13th Lunar Planet. Sci. Conf.* (1982), p. 580; J. S. Gilmore, J. D. Knight, C. J. Orth, C. L. Pillmore, R. H. Tschudy, *Nature (London)*, in press.
3. J. Smit and W. G. H. Z. ten Kate, *Cretaceous Res.* **3**, 307 (1982).
4. G. W. Wetherill and E. M. Shoemaker, *Geol. Soc. Am. Spec. Pap. 190* (1982), p. 1, and references therein; P. R. Weissman, *ibid.*, p. 15; R. A. F. Grieve, *ibid.*, p. 25.
5. D. M. Raup and J. J. Sepkoski, Jr., *Science* **215**, 1501 (1982).
6. R. Ganapathy, *ibid.* **216**, 885 (1982); *Geol. Soc. Am. Spec. Pap. 190* (1982), p. 513.
7. W. Alvarez, F. Asaro, H. V. Michel, L. W. Alvarez, *Science* **216**, 886 (1982).
8. F. Asaro, L. W. Alvarez, W. Alvarez, H. V. Michel, *Geol. Soc. Am. Spec. Pap. 190* (1982), p. 517.
9. A. R. Palmer, *ibid.*, p. 469.
10. J. H. Stitt, *J. Paleontol.* **45**, 178 (1971).
11. R. K. Bambach, C. R. Scotese, A. M. Ziegler, *Am. Sci.* **68**, 26 (1980).
12. We thank the Los Alamos National Laboratory Reactor Group for performing the neutron irradiations and for deriving some of the elemental data with their automated system. We thank P. Boni for preparing thin sections and oriented slabs of the critical boundary intervals. This research was supported by the Department of Energy.

7 September 1983; accepted 13 October 1983

Seismic Detection of the Summit Magma Complex of Kilauea Volcano, Hawaii

Abstract. *Application of simultaneous inversion of seismic P-wave arrival time data to the investigation of the crust beneath Kilauea Volcano yields a detailed picture of the volcano's heterogeneous structure. Zones of anomalously high seismic velocity are found associated with the volcano's rift zones. A low-velocity zone at shallow depth directly beneath the caldera coincides with an aseismic region interpreted as being the locus of Kilauea's summit magma complex.*

For a number of years the Hawaiian Volcano Observatory (HVO) has operated a seismic network to monitor the thousands of earthquakes that occur annually beneath Kilauea Volcano and the surrounding region. These earthquakes are caused by the volcanic and tectonic forces that build and shape the shield volcanoes of Hawaii. The seismic activity provides a means of probing the deep structure of Kilauea. For example, the spatial distribution of magma-related seismic events has been used to map the structure of Kilauea's magmatic passageways (*1, 2*). Furthermore, an aseismic zone directly beneath the Kilauea caldera has been interpreted as being the volcano's summit magma reservoir (*1*).

Seismic wave travel time has also been utilized to map the subsurface structure of Kilauea, both with refraction (*3, 4*) and teleseismic (*5*) data. All these studies provide clear evidence for the laterally heterogeneous seismic velocity structure of the crust beneath Kilauea. This report presents a three-dimensional model for the P-wave velocity structure of the crust beneath Kilauea, determined by the inversion of local earthquake P-wave arrival times recorded by the HVO seismic network. The data set and method used permit the resolution of structure on a spatial scale of 3 to 4 km. Extreme lateral variations in velocity are revealed, particularly in the contrast between nonrift (relatively low velocities) and rift and summit areas (high velocities). In addition, a zone of low velocity is detected that coincides with the aseismic region beneath the caldera, confirming this to be a zone of low rigidity.

The use of local earthquake arrival time data to determine a model for three-dimensional seismic structure has proved successful in probing the earth's crust and upper mantle (*6–10*). In early studies of this type a method was used that involves simultaneous inversion for earthquake locations and velocity structure in a single step (*6*). Two recently developed techniques have made iterative three-dimensional inversion practical. One is parameter separation (*7, 11*), a procedure for decomposing the simultaneous inversion problem into a set of equations involving velocity model perturbations only. As a result, the computational size of the inversion problem can be kept manageably small no matter how many earthquakes are included. The second is approximate ray tracing (ART) (*8, 9, 12*), which takes advantage of Fermat's principle to derive approximate ray paths and travel times in an arbitrary velocity structure. ART is far faster computationally than existing three-dimensional ray tracing algorithms, making it practical to determine an iterative solution to the nonlinear simultaneous inversion problem. Both parameter sepa-